Progress in Biophysics and Molecular Biology 107 (2011) 456–463

Contents lists available at SciVerse ScienceDirect

Progress in Biophysics and Molecular Biology

journal homepage: www.elsevier.com/locate/pbiomolbio

Review

Evaluation and characterization of fetal exposures to low frequency magnetic fields generated by laptop computers

Nicola Zoppetti [a,*], Daniele Andreuccetti [a], Carlo Bellieni [b], Andrea Bogi [c], Iole Pinto [c]

[a] CNR, Institute of Applied Physics "Nello Carrara" (IFAC-CNR), Via Madonna del Piano 10, 50019 Sesto Fiorentino (FI), Italy
[b] Department of Paediatrics, Obstetrics and Reproduction Medicine, University of Siena, Siena, Italy
[c] ASL 7, Prevention Department, Physical Agents Laboratory, Siena, Italy

ARTICLE INFO

Article history:
Available online 15 October 2011

Keywords:
Laptop computers
Fetal exposures
Low frequency
Magnetic field
Numerical dosimetry

ABSTRACT

Portable – or "laptop" – computers (LCs) are widely and increasingly used all over the world. Since LCs are often used in tight contact with the body even by pregnant women, fetal exposures to low frequency magnetic fields generated by these units can occur. LC emissions are usually characterized by complex waveforms and are often generated by the main AC power supply (when connected) and by the display power supply sub-system.

In the present study, low frequency magnetic field emissions were measured for a set of five models of portable computers. For each of them, the magnetic flux density was characterized in terms not just of field amplitude, but also of the so called "weighted peak" (WP) index, introduced in the 2003 ICNIRP Statement on complex waveforms and confirmed in the 2010 ICNIRP Guidelines for low frequency fields. For the model of LC presenting the higher emission, a deeper analysis was also carried out, using numerical dosimetry techniques to calculate internal quantities (current density and in-situ electric field) with reference to a digital body model of a pregnant woman. Since internal quantities have complex waveforms too, the concept of WP index was extended to them, considering the ICNIRP basic restrictions defined in the 1998 Guidelines for the current density and in the 2010 Guidelines for the in-situ electric field. Induced quantities and WP indexes were computed using an appropriate original formulation of the well known *Scalar Potential Finite Difference* (SPFD) numerical method for electromagnetic dosimetry in quasi-static conditions.

Contents

* Corresponding author. Tel.: +39 055 5226446; fax: +39 055 5226459.
E-mail address: n.zoppetti@ifac.cnr.it (N. Zoppetti).

0079-6107/$ – see front matter © 2011 Elsevier Ltd. All rights reserved.
doi:10.1016/j.pbiomolbio.2011.10.003

1. Introduction

USL7-Siena and IFAC-CNR, with the collaboration of the University of Siena, are cooperating in a project aimed at assessing exposures to electromagnetic fields in occupational environments. One of the objectives of the project is to create and populate a Database, called “Physical Agent Portal”, in which the main sources of occupational exposures are represented. In offices and especially in domestic environments laptop computers can be used by pregnant women in tight contact with the body (see Fig. 1), and even with the womb. Laptop computers (LC) and their battery chargers (BT) are sources of considerable magnetic fields, with frequency contents that can vary depending on the model and the considered zone of the device. In any case the magnetic field has an impulsive or, more generally, a complex (i.e. not sinusoidal) waveform. Five models of LC and BT were considered and preliminary magnetic flux density measurements were carried out to find the points characterized by the maximum field intensity, both close to the laptop and close to the battery charger. Then the field was measured and acquired in those 10 points. The collected samples were elaborated to apply the weighted peak (WP) approach and to obtain a set of WP indexes whose values ‘indicate’ – if greater than 1 – that the corresponding exposure standard has been exceeded. This step entailed the development of numerical filters that represent the inverse of the pertinent ICNIRP reference levels. For the model of laptop that generates the higher WP indexes a dosimetric analysis was also carried out, assuming the impressed magnetic field was uniform in the volume occupied by the pregnant digital body model and equal to the field measured close to the device. This deepening in dosimetric sense was executed also for the battery charger that generates the higher exposure indexes.

In general, in this work it is shown how it is possible to assess exposures taking into account the complete waveforms of the pertinent induced quantities, rather than just using some summarizing parameters like RMS or peak values, which are poorly descriptive when complex waveforms are involved. On the other hand, it is also shown how the weighted peak approach applied to basic restrictions represents a convenient way to verify compliance to exposure standards and to express the exposure characteristics with a single parameter even from a dosimetric point of view.

While the complexity of the time dependency of the impressed field was fully considered in the dosimetric analysis, for what concerns its spatial distribution, the field was supposed to be homogeneous (with the maximum detected field amplitude). Thanks to this approach, a clearer description of the method presented in the work was possible. In any case, this approach do not invalidate the comparison of weighted peak indexes obtained according to the old (1998) and the new (2010) ICNIRP Guidelines. On the other hand, the results of this kind of analysis are significant only in case of compliance with the guidelines, since the considered field intensity is much higher than the real one in almost the entire volume occupied by the exposed subject. If a non-compliant situation should arise, a more detailed analysis would be necessary, representing the actual spatial distribution of the impressed field.

2. Materials and methods

2.1. Selected laptops

The five LCs listed in Table 1 were considered in this study together with their BTs. In the same table, an identification tag from ‘A’ to ‘E’ was attached to every model, that will be used to identify the particular model in the rest of the paper.

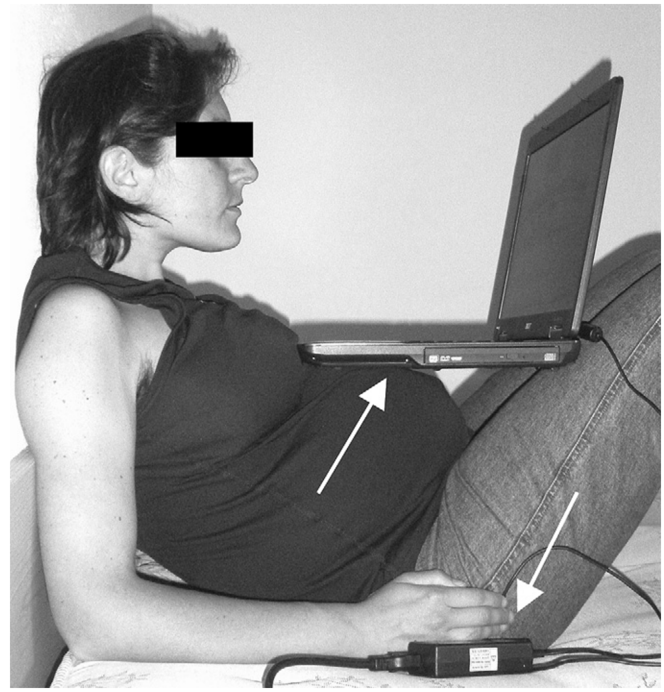

Fig. 1. ‘Laptop’ use of a laptop computer in pregnancy. The arrows indicate the laptop and its battery charger.

Table 1
Laptops under test.

ID	Model
A	Acer Aspire 5920
B	Dell Inspiron 610M
C	Dell Precision M4400
D	Sony Vaio vgnz41md
E	Apple Macbook Pro

2.2. Measurement setup

To measure and acquire the magnetic field waveforms, the acquisition chain represented in Fig. 2 was used. This is composed by a Narda ELT-400 Exposure Level Tester (Narda Safety Test Solutions, Pfullingen, Germany) that makes available three analog outputs proportional to the Cartesian components of the measured field. These outputs were sampled with an Agilent U2531A Data Acquisition Device (Agilent Technologies, USA) and then stored on a standard PC connected to the U2531A through a USB interface. As represented in the block diagrams of Fig. 3, the ELT-400 can be used in two distinct operational modes. The first mode, the so called “Field Strength” mode (on the left in Fig. 3) is characterized by a flat response between few Hz and 400 kHz.

The block diagram on the right in Fig. 3 implements the so called “Shaped Time Domain” mode and uses three analog filters

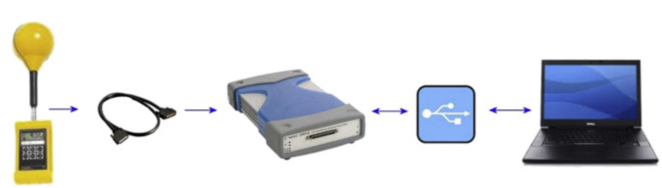

Fig. 2. Measurement setup.

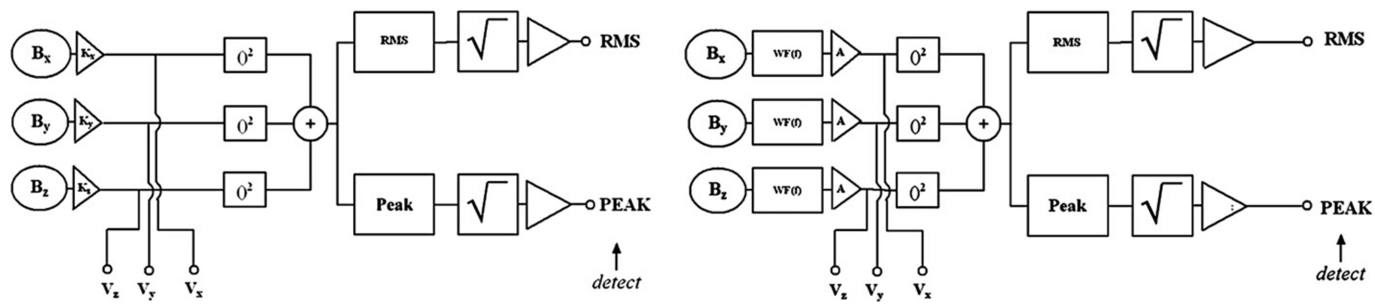

Fig. 3. Narda ELT-400 block diagrams, Field Strength mode (left), Shaped Time Domain mode (right).

(upstream of the analog outputs) whose amplitude responses follow the inverse of the ICNIRP reference levels.

This is a hardware implementation of the so called "Weighted Peak" approach, that was introduced in the 2003 ICNIRP statement on complex waveforms (ICNIRP, 2003). This approach leads to determine some exposure indexes (that will be called WP03 for 1998 Guidelines and WP10 for 2010 Low Frequencies Guidelines in the following). These indexes should be used in all the cases in which it is not possible to approximate the signal with a simple sinusoidal waveform whose RMS amplitude has to be compared with the reference level at the appropriate frequency. In the present study we decided to measure the fields in "Field Strength" mode and to apply the weighted peak approach on a software basis, as a post-measurement step. This is also motivated by the fact that in this way it is possible to use the same measured values to calculate weighted peak indexes according to different exposure standards.

2.3. Numerical implementation of 'ICNIRP filters'

The reference levels for general population defined in ICNIRP (1998) will be considered in order to present how the 'ICNIRP filters' were developed. Fig. 4 and equation (1) refer to the analog implementation of the filter that follows the inverse of those reference levels. Equation (2) represents the transfer function of the corresponding digital filter, synthesized using the standard technique called *zero-pole matching* (Oppenheim and Shafer, 2010).

$$\begin{aligned} H_c(s) &= A_f \frac{s^2}{(s+a)(s+b)} \\ A_f &= \frac{1}{6.25 \cdot 10^{-6}\sqrt{2}} \\ a &= 2\pi \cdot 8Hz \quad b = 2\pi \cdot 800Hz \end{aligned} \tag{1}$$

In equation (2) T_c is the sampling interval and f_n is a normalization frequency (at which the transfer functions of the analog and the numerical filters have the same amplitude) that in the present study was chosen equal to 1/200 of the sampling rate $1/T_c$.

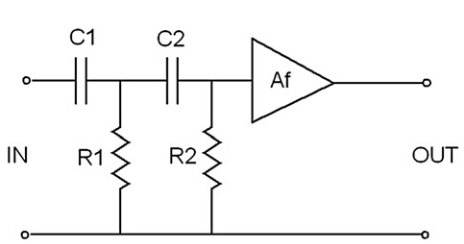

Fig. 4. Analog implementation of the inverse of ICNIRP (1998) reference levels for general population, where a = 1/(R1C1) and b = 1/(R2C2).

$$\begin{aligned} H_d(z) &= A_f \cdot K \cdot \frac{1 - 2\cdot z^{-1} - z^{-2}}{1 - (a1 + b1)z^{-1} + a1 \cdot b1 \cdot z^{-2}} \\ a1 &= e^{-j2\pi a T_c} \quad b1 = e^{-j2\pi b T_c} \\ K &= \left| \frac{H_c(s = j2\pi f_n)}{H_d\left(z = e^{j2\pi f_n T_c}\right)} \right| \end{aligned} \tag{2}$$

Comparing the amplitude and the phase responses of the analog and the numerical filters, a good agreement can be observed at 'low' frequencies that becomes worst getting closer to the so called Nyquist limit $1/(2T_c)$. This is more evident for the phase which is always zero at the Nyquist limit for the numerical filter. In Table 2, the percentage relative differences of the amplitudes and of the phases of the numerical and analog filters are reported. Looking at the phase column, it is clear how it is necessary to use a sampling frequency '*sufficiently*' higher than the highest significant component of the input spectrum. This could request a preliminary acquisition at the maximum available sampling rate and a subsequent spectral analysis, if the characteristics of the measured field are not known before the measurement campaign.

2.4. Basics of the dosimetric method

As it will be presented in the 'Results' section, the measured field is characterized by a complex waveform. In this case, the standard dosimetric methods in the frequency domain are not a convenient choice, unless the impressed field spectrum is composed by a few significant frequencies. After a preliminary study, four basic requirements were devised for the dosimetric method to be used. (1) First of all, the attention was focused on the time evolution of the exposures and not on the space distribution of the field. As a consequence, the impressed field was considered uniform in the volume occupied by the body model of the pregnant woman. (2) The method had to be suitable to treat exposures to complex waveform impressed fields with general polarization. (3) The method should avoid the spectral decomposition of the waveforms (not convenient in case of several spectral components and in relation to the so called "spectral leakage" phenomenon) (Harris, 1978). (4) The method should allow assessing of compliance with ICNIRP basic restrictions that vary with frequency through the

Table 2
Percentage relative differences of the amplitudes and of the phases between the numerical and analog transfer functions.

	Δ% (amplitude)	Δ% (phase)
Fs/8	0.004%	5.3
Fs/4	0.021%	21.6
Fs/2	0.130%	100.0

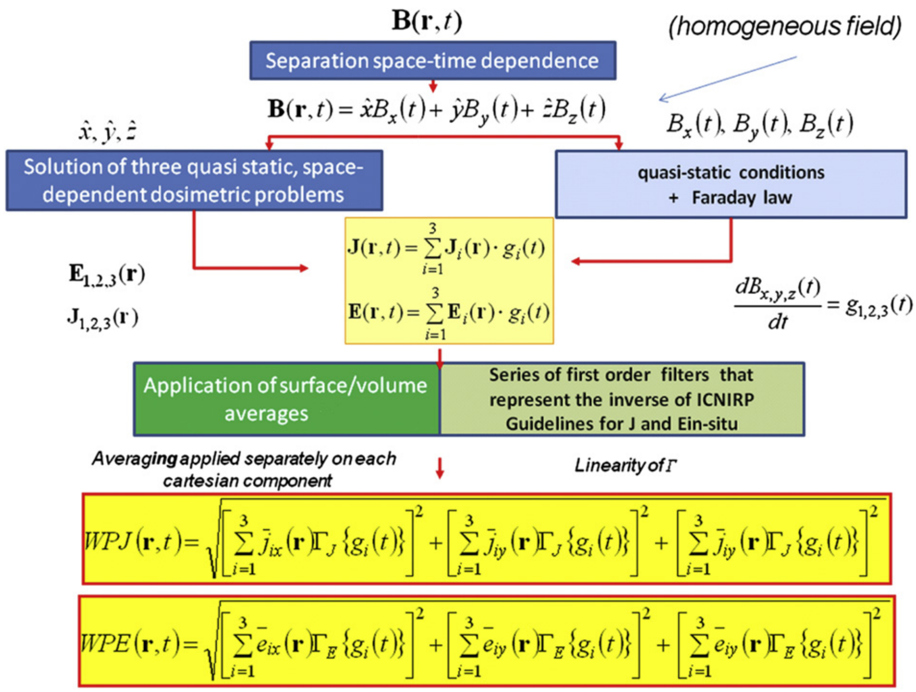

$$\mathbf{J}(\mathbf{r},t)=\sum_{i=1}^{3}\mathbf{J}_i(\mathbf{r})\cdot g_i(t)$$

$$\mathbf{E}(\mathbf{r},t)=\sum_{i=1}^{3}\mathbf{E}_i(\mathbf{r})\cdot g_i(t)$$

$$WPJ(\mathbf{r},t)=\sqrt{\left[\sum_{i=1}^{3}\bar{j}_{ix}(\mathbf{r})\Gamma_J\{g_i(t)\}\right]^2+\left[\sum_{i=1}^{3}\bar{j}_{iy}(\mathbf{r})\Gamma_J\{g_i(t)\}\right]^2+\left[\sum_{i=1}^{3}\bar{j}_{iy}(\mathbf{r})\Gamma_J\{g_i(t)\}\right]^2}$$

$$WPE(\mathbf{r},t)=\sqrt{\left[\sum_{i=1}^{3}\bar{e}_{ix}(\mathbf{r})\Gamma_E\{g_i(t)\}\right]^2+\left[\sum_{i=1}^{3}\bar{e}_{iy}(\mathbf{r})\Gamma_E\{g_i(t)\}\right]^2+\left[\sum_{i=1}^{3}\bar{e}_{iy}(\mathbf{r})\Gamma_E\{g_i(t)\}\right]^2}$$

Fig. 5. Schematic representation of the dosimetric method.

definition of a weighted peak index referred to the same ICNIRP restrictions.

In the scheme of Fig. 5 a 'logical block diagram' of the developed method is illustrated; it is based on the separation of the main problem into the time- and the spatial-dependent components. This separation is immediate in case of linear polarization of the impressed field (not necessarily uniform). With a uniform field with general polarization, it is opportune to split the problem into three linearly polarized problems, one for each Cartesian component of the impressed field. Since coupling of the magnetic flux density with the human body at low frequency is governed by the Faraday law, the time dependent part of each of the three problems entails the calculation of a simple time derivative (in Fig. 5, the three functions $g_i(t)$ are adimensional and represent the time dependency of the time derivative of the three Cartesian components of the magnetic flux density). On the 'spatial side', the solution of three different dosimetric problems is necessary, using a quasi-static technique like the Scalar Potential Finite Difference method (Andreuccetti and Zoppetti, 2006). The amplitude of the impressed field can be chosen without reference to the real one, since the actual solution is built up in a post-processing step (in the present case, three impressed field of 1 T, parallel to the three reference Cartesian axes were considered separately).

After this first step has been completed, on both the time and spatial sides, it is possible to calculate the induced quantities E and J in every instant in which the impressed field was measured.

To achieve the objective of calculating weighted peak indexes referred to basic restrictions, a second step is necessary on both the parts in which the problem was divided. On the spatial side, the solutions of the three dosimetric problems relative to the three Cartesian components have to be spatially averaged over a surface of 1 cm^2 (ICNIRP, 1998) or on a volume of $2 \times 2 \times 2$ mm^3 (ICNIRP, 2010). On the other side, the three time derivatives of the Cartesian components of the impressed field have to be weighted with a digital filter that implements the inverse of the basic restrictions we are referring to. In Fig. 5, the action of the filter is represented with a functional Γ_J or Γ_E. Results of spatial and temporal processing can finally be composed to obtain the desired indexes WPJ and WPE. This is possible thanks to the linearity of the filter and to the application of spatial average on each Cartesian component separately (Zoppetti and Andreuccetti, 2009).

2.4.1. *The choice of a reference frequency or of a reference conductivity*

An important detail, not discussed in the previous paragraph, is how each tissue can be assigned a particular value for conductivity. This can be done in a direct or indirect way. The direct way entails that the frequency trend of conductivity in the frequency span occupied by the spectrum of the (derivative of the) impressed field is integrated (and possibly weighted) over the frequency span itself, to obtain a single value for each tissue to be used in the dosimetric analysis. The indirect way consists in finding a 'reference frequency' and in using the Gabriels's parametric model (Gabriel et al., 1996) to calculate the tissue conductivities at that frequency.

In this paper the indirect approach was used and the calculation of the reference frequency was based on the spectrum of the quantity of interest. For example, aiming at calculating WPJ or WPE, the three waveforms $\Gamma_{J \text{ or } E}\{g_i(t)\}$ $(i = 1, 2, 3)$ were considered, then their DFTs were calculated on a time frame with a suitable length to obtain a sufficient spectral resolution (0.5 s → 2 Hz in the present cases). For each spectral component, the RSS of the three indexes $\Gamma_{J \text{ or } E}\{g_i(t)\}$ was calculated. The frequency at which this quantity achieves its maximum was adopted as the reference frequency.

2.5. *The pregnant body model*

The pregnant body model used in this study is described in Nagaoka et al. (2007). In this paper the pregnant woman model, excluding the fetus and surrounding tissues, was developed by deforming a high-resolution whole body voxel model of an adult Japanese female on the basis of MRI data collected from a non-

Table 3
Measured magnetic flux densities/indexes under the laptops.

Laptop (LC)				
	Bmax [μT]	Brms [μT]	WP03max	WP10max
A	2.11	0.738	0.221	0.042
B	5.27	0.931	0.233	0.033
C	2.88	1.08	0.143	0.015
D	1.79	0.547	0.141	0.032
E	2.49	0.991	0.188	0.042

Table 4
Measured magnetic flux densities/indexes close to the battery chargers.

Battery charger (BT)				
	Bmax [μT]	Brms [μT]	WP03max	WP10max
A	30.2	4.73	1.75	0.225
B	20.0	2.74	1.12	0.142
C	10.5	2.70	0.868	0.165
D	3.61	1.30	0.292	0.052
E	0.687	0.281	0.045	0.011

pregnant Japanese woman. This model was segmented with a spatial resolution of 2 mm and was classified into 51 different tissues and organs. The abdominal skin, fat and muscle tissues were dilated to match the abdominal shape at 26 weeks of pregnancy; next, the woman model was combined with the fetal model to obtain the pregnant woman model consisting of about 7 million 2 mm cubical voxels, classified into 56 tissues and organs. The fetal model was constructed on the basis of abdominal magnetic resonance imaging (MRI) data of a 26-week-pregnant woman. It was classified into six different types of tissue, namely: fetal eyes, fetal brain, fetal body, amniotic fluid, placenta and uterine wall. The conductivities of the three fetal tissues were derived using the ones of eyes and brain and a weighted average over all the tissue conductivities of the Virtual Family children voxel phantoms (Christ et al., 2010) increased by 10% (Cech et al., 2007) respectively. This increase takes into account for the higher water content of fetal tissues. In agreement with the Nagaoka et al. model, the dielectric properties of the amniotic fluid were taken equal to the ones of the cerebro spinal fluid.

3. Results and discussion

3.1. Measured fields and comparison with ICNIRP reference levels in terms of weighted peak indexes

In Tables 3 and 4 some summarizing parameters of the measured values are reported, referring to the five models of LCs and BTs respectively.

The samples of the impressed field intensities were measured and recorded using sampling rates of 200 kS/ch/s (LCs) and 50 kS/ch/s (BTs). These values were chosen as a compromise between bandwidth (with respect to the field spectrum) and file size. As it can be noted, excepted the model E, battery chargers are the sources of higher fields, both in terms of absolute amplitudes and rms values and in terms of weighted peak indexes.

In Fig. 6 the plot of the measured field is reported for LC, model A (on the left), together with its polarization (center) and spectrum (right). Fig. 7 is equivalent to Fig. 6 but is referred to BT, model A. In the latter figure, it can be noted that the spikes in the time domain are 10 ms apart (i.e. half period of the 50 Hz sinusoid). This periodicity results in a spectrum that is composed by 100 Hz spaced lines.

Looking at the spectra of Figs. 6 and 7, it is evident how in these cases the spectral decomposition of the problem would have been extremely onerous.

In Table 5, the reference frequencies used to assign conductivities are reported in the case of LP and BT, model A (calculated as explained in the paragraph 2.4.1). As it can be noted, in general, different reference frequencies are used for the calculation of different quantities induced by the same impressed field.

3.2. Results of the dosimetric study referred to the laptop (model A)

A dosimetric analysis was carried out referring to model A LC. In Table 6 the maximum and the 99-percentile of the dosimetric quantities are reported for various tissues and the maximum values are evidenced in bold for every column. These values are useful to understand the order of magnitude of the phenomenon, but are poorly descriptive in case of complex waveforms, since there is no information about the involved frequencies. On the contrary, Tables 7, 8 and 9, show results in terms of weighted peak indexes and integrate the information about the complex waveforms of the induced quantities, weighted according to the proper ICNIRP Basic Restrictions, which vary with frequency.

The results of Table 7 were calculated taking into account a surface average on 1 cm^2 of the current density with the so called 'full-averaging' approach (Zoppetti and Andreuccetti, 2009) (since the voxel size is 2 mm, the spatial averaging was actually possible).

With regard to the column containing the maximum values, it can be noted that the maximum exposure in mother's CNS is located in the spinal chord and reaches the 15% of the current density basic restriction (the Cerebro Spinal Fluid is not considered part of CNS). In the fetus, the WPJ index is almost 13% the basic restriction. So, in this case, the indexes are much lower than the unity even with a greatly overestimated exposure, supposed uniform on the entire body model.

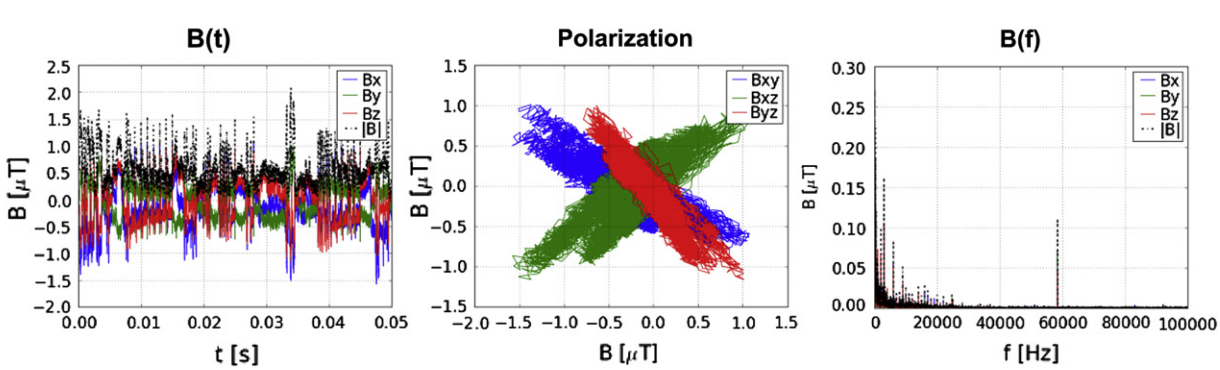

Fig. 6. Magnetic flux density measured under laptop A.

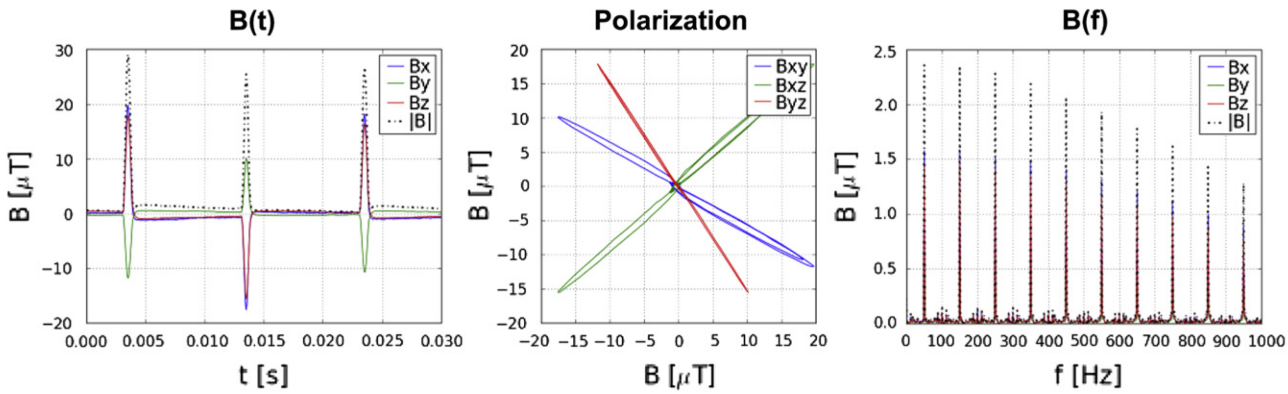

Fig. 7. Magnetic flux density measured close to battery charger A.

The results of Tables 8 and 9 refer to the 2010 LF ICNIRP guidelines that prescribe to consider the induced electric field instead of current density and to average on a cube with a 2 mm side. Since 2 mm is also the voxel size, in this case the averaging was not applied. Even if the ICNIRP guidelines are not completely clear on that aspect, in this case (where the impressed field is taken as homogeneous) the 99-percentile on every tissue of the WPE index was considered as the reference quantity. It must be noted that this approach would probably have less sense in the case of a non-homogeneous impressed field, since not all the voxels composed by the same given tissue were exposed to the same field and any percentile would depend also on the number of voxels exposed to a negligible field level. This is particularly true in case of partial body exposure, in which the 99-percentile criteria introduced to define the peak electric field in the tissues should be referred just to the exposed part of the body. On the other hand, in this case the concept of "partial body exposure" should be quantitatively defined and the new ICNIRP guidelines do not help on this aspect (but any possible definition may appear as arbitrary).

The results in terms of WPE indexes are reported in two distinct tables since different limits apply to tissues of the head belonging to the central nervous system (CNS, Table 9) and to all other tissues (PNS, Table 8).

For the fetus the more restrictive limits were applied; for this reason fetal tissues appear in Table 8. Comparing Tables 7, 8 and 9 it can be noted that the WPE index is much lower than the WPJ in the same tissue (and for the same exposure conditions).

3.3. Results of the dosimetric study referred to the battery charger (model A)

A dosimetric study was also carried out on the exposure due to the model A battery charger. The results in terms of weighted peak indexes are reported here. As the WP03 and WP10 indexes were much higher than in the LC case, also higher WPJ and WPE indexes were expected. This is what effectively happened, as shown in Tables 10, 11 and 12.

In Table 10 a WPJ index exceeding 1 can be noted in the brain gray matter, in the spinal chord (mother CNS) and in the fetus. In this case a more refined analysis would be appropriate, taking into account the spatial in-homogeneity of the impressed field.

A possible violation of the ICNIRP rationale seems to happen in the spinal chord, since the WPJ index (1.905) is higher than the WP03 index (1.75).

When we speak about "violation of the ICNIRP rationale", we are NOT signalizing a lack of compliance with ICNIRP guidelines. On the contrary, almost all the situations we are describing are compliant with the guidelines, considering that even if we have greatly overestimated the exposure (taking the field as homogeneous), the weighted peak indexes for the internal quantities are less than 1.0. What we want to highlight is a situation that pick out a possible internal inconsistency of the guidelines. In fact, the ICNIRP guidelines are based on a fundamental assumption (which in turn should rely on the use of highly precautionary dosimetric models). According to this assumption, compliance with reference levels should guarantee compliance with basic restrictions. In other words, if one measures the electric and magnetic fields and find them lower than the corresponding reference levels, he/she should be *assured* that the basic restrictions are not exceeded. Considering the weighted peak indexes, this assumption implies that the reference level indexes must always result higher than the basic restriction indexes.

In the previously evidenced case (WPJ in spinal chord, Table 10), this inconsistency is probably due to the so called 'full-averaging'

Table 5
Reference frequencies.

f_0 [Hz]		
	LC-A	BT-A
J/*E*	58,440	850
WPJ	3000	750
WPE	58,440	150

Table 6
In-situ electric fields and current densities induced by the magnetic field generated by model A LC.

LC-A				
Tissue name	*E* [V/m] max	*E* [V/m] 99%-ile	*J* [A/m^2] max	*J* [A/m^2] 99%-ile
Bone cortical	0.120	0.050	0.0025	0.0010
Brain gray matter	0.050	0.017	0.0064	0.0021
Brain white matter	0.032	0.015	0.0025	0.0011
Cerebellum	0.019	0.010	0.0028	0.0015
Cerebro spinal + amniotic fluid	0.020	0.010	0.0404	0.0194
Fat	0.168	0.037	0.0041	0.0009
Spinal chord	0.050	0.019	0.0036	0.0014
Bone cancellous	0.111	0.039	0.0048	0.0017
Pons	0.009	0.005	0.0009	0.0005
Muscle	0.093	0.018	0.0329	0.0064
Skin	0.521	0.034	0.0094	0.0006
Fetal brain	0.034	0.010	0.0039	0.0012
Fetal eye	0.004	0.003	0.0058	0.0047
Fetus (all other tissues)	0.058	0.020	0.0019	0.0007

Table 7
WPJ indexes in CNS, fetus and other tissues, induced by the magnetic field generated by model A LC.

WPJ–LC-A					
Tissue name	Max	Average	Median	1%-ile	99%-ile
Brain gray matter	0.094	0.010	0.007	0.001	0.049
Brain white matter	0.050	0.005	0.004	0.001	0.013
Cerebellum	0.071	0.009	0.007	0.002	0.044
Cerebro spinal + amniotic fluid	0.249	0.096	0.096	0.007	0.200
Spinal chord	0.153	0.019	0.007	0.000	0.112
Pons	0.033	0.003	0.002	0.001	0.016
Fetal brain	0.014	0.007	0.007	0.004	0.009
Fetal eye	0.021	0.010	0.010	0.002	0.020
Fetus (all other tissues)	0.129	0.007	0.002	0.000	0.066

Table 8
WPE–PNS indexes in fetus and other tissues induced by the magnetic field generated by model A LC.

WPE–PNS–LC-A					
Tissue name	Max	Average	Median	1%-ile	99%-ile
Bone cortical	0.030	0.003	0.002	0.000	0.012
Cerebro spinal + amniotic fluid	0.005	0.001	0.001	0.000	0.002
Fat	0.043	0.003	0.002	0.000	0.010
Ovary	0.006	0.002	0.002	0.001	0.004
Spinal chord	0.012	0.001	0.001	0.000	0.005
Uterus	0.011	0.002	0.002	0.000	0.004
Bone cancellous	0.028	0.002	0.002	0.000	0.010
Lung	0.007	0.001	0.001	0.000	0.004
Muscle	0.024	0.001	0.001	0.000	0.004
Skin	0.150	0.002	0.002	0.000	0.009

algorithm, according to which the surface average in spinal chord includes voxels composed by the liquor, which has a high conductivity and is consequently characterized by high values of current density.

The values of WPE index are much lower than WPJ (especially if the 99-percentile is considered) and never exceed unity. Another possible violation of ICNIRP rationale is detected in the skin (Table 11), in which a maximum value (0.631) much higher than the 99-percentile (0.039) can be noted (WP10 is 0.042 so in this case is not really an inconsistency). This peak is also evident in Fig. 8 that represents the maximum of WPE (right) and WPJ (left) indexes calculated on each axial section.

As it can be noted, the peak of the WPE index observed in Table 11 is located in the upper part of the legs of the pregnant woman. A close examination showed that the peak is reached where a skin-to-skin contact of the two thighs occurs. In general, the induced electric field tends to be high in the skin, due to the low conductivity of this tissue (with respect to the surrounding ones) and to the fact that it is a peripheral tissue (the fields induced by an external magnetic field tend to be higher at the margin of the 'effective' surface perpendicular to the external field itself).

If the 99-percentile is considered, the ICNIRP rationale is not violated, since the WPE index in the skin (0.039) is lower than WP10 (0.225), but this is not true if the maximum of WPE in the skin is taken into account (0.631). In the case of the BT a comparison of the weighted peak exposure indexes is proposed in Table 13. As it can be noted the ratio WP03/WP10 is almost 8.

This is not surprising if Fig. 9 and the spectrum of Fig. 7 are taken into account. It should be noted also that the average value of the ratio WPJ/WPE is more than 36, meaning that in this situation the new guidelines allow exposures almost 40 times higher than the old ones. Considering the maximum of WPE and not the 99-percentile, that ratio would decrease to less than 28.

Table 9
WPE–CNS indexes in CNS (head) and fetal tissues, induced by the magnetic field generated by mod. A LC.

WPE–CNS–LC-A					
Tissue name	Max	Average	Median	1%-ile	99%-ile
Brain gray matter	0.013	0.001	0.001	0.000	0.004
Brain white matter	0.008	0.001	0.001	0.000	0.004
Cerebellum	0.005	0.001	0.001	0.000	0.003
Pons	0.002	0.000	0.000	0.000	0.001
Fetal brain	0.008	0.002	0.002	0.001	0.003
Fetal eye	0.001	0.000	0.000	0.000	0.001
Fetus (all other tissues)	0.014	0.002	0.001	0.000	0.005

Table 10
WPJ indexes in CNS, fetus and other tissues, induced by the magnetic field generated by the battery charger of notebook A.

WPJ–BT-A					
Tissue	Max	Average	Median	1%-ile	99%-ile
Brain gray matter	1.209	0.125	0.090	0.013	0.620
Brain white matter	0.643	0.057	0.049	0.008	0.162
Cerebellum	0.875	0.116	0.088	0.032	0.552
Cerebro spinal + amniotic fluid	3.142	1.206	1.207	0.094	2.501
Fat	1.228	0.050	0.035	0.005	0.259
Spinal chord	1.905	0.237	0.085	0.002	1.394
Pons	0.430	0.034	0.022	0.009	0.207
Muscle	1.411	0.228	0.195	0.020	0.703
Skin	0.485	0.010	0.007	0.000	0.048
Fetal brain	0.168	0.085	0.085	0.049	0.119
Fetal eye	0.266	0.136	0.134	0.024	0.255
Fetus (all other tissues)	1.608	0.093	0.030	0.004	0.847

Table 11
WPE–PNS indexes in fetus and other tissues, induced by the magnetic field generated by the battery charger of notebook A.

WPE–PNS–BT-A					
Tissue	Max	Average	Median	1%-ile	99%-ile
Bone cortical	0.118	0.010	0.007	0.001	0.049
Cerebro spinal + amniotic fluid	0.021	0.005	0.005	0.001	0.010
Fat	0.176	0.012	0.010	0.002	0.039
Spinal chord	0.062	0.005	0.003	0.001	0.024
Uterus	0.046	0.008	0.008	0.001	0.017
Bone cancellous	0.110	0.009	0.006	0.001	0.040
Muscle	0.098	0.006	0.005	0.001	0.018
Skin	0.631	0.011	0.009	0.001	0.039

Table 12
WPE–CNS indexes in CNS (head) and fetal tissues, induced by the magnetic field generated by the battery charger of notebook A.

WPE–CNS–BT-A					
Tissue	Max	Average	Median	1%-ile	99%-ile
Brain gray matter	0.103	0.011	0.010	0.001	0.033
Brain white matter	0.065	0.011	0.009	0.002	0.028
Cerebellum	0.037	0.009	0.008	0.002	0.019
Pons	0.015	0.004	0.003	0.001	0.009
Fetal brain	0.059	0.013	0.013	0.009	0.020
Fetal eye	0.005	0.002	0.002	0.000	0.005
Fetus (all other tissues)	0.097	0.011	0.010	0.002	0.034

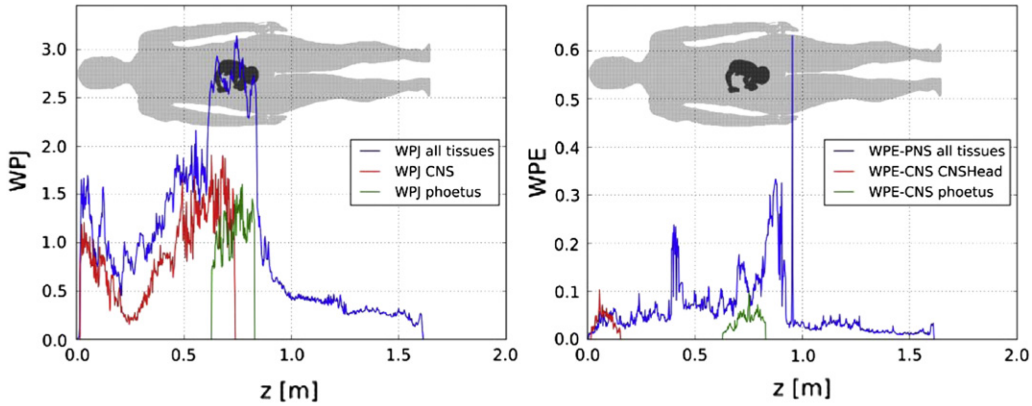

Fig. 8. WPE (left) and WPJ (right) indexes 'induced' by the magnetic field generated by the battery charger of notebook A: maximum on each axial section.

Table 13
Comparison of ICNIRP (1998) (WP03/WPJ) and ICNIRP (2010) (WP10/WPE) exposure indexes (BT, model A).

Tissue	WP03	WP10	WP03/WPJ	WPJ max	WPE–CNS 99%	WPJ/WPE
Brain gray matter	1.75	0.225	7.78	1.21	0.033	36.7
Brain white matter				0.64	0.028	22.9
Cerebellum				0.87	0.019	45.8
Pons				0.43	0.009	47.8
Fetal brain				0.17	0.020	8.5
Fetal eye				0.27	0.005	54.0
Fetus (all the other)				1.61	0.034	47.4

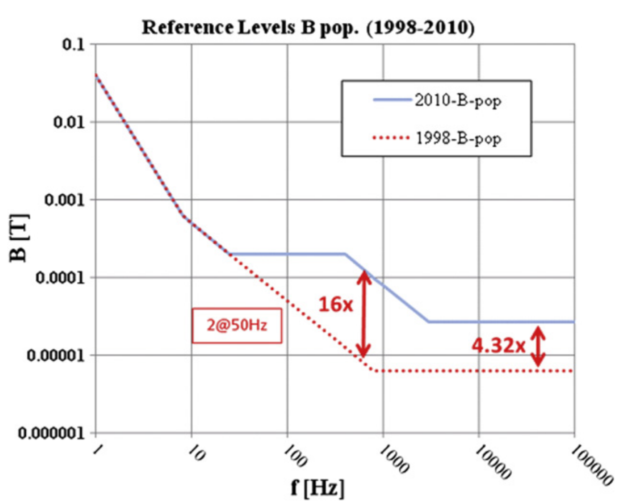

Fig. 9. Comparison of ICNIRP (1998) and ICNIRP (2010) reference levels for general population.

4. Conclusions

A possible approach to the evaluation of exposures to complex waveform magnetic fields was presented and applied to the particular case of the fetal exposure to the magnetic flux density generated by five models of laptop computers and their battery chargers. The analysis showed that for 4 models, the BTs generate higher exposure indexes than the corresponding LCs.

Particular attention was focused on the calculation of the so called WPJ and WPE indexes, that implement the weighted peak approach, which is particularly well suited when checking compliance with basic restrictions in case of complex waveforms.

Even using a greatly overestimated exposure (the field is supposed uniform in the whole body model volume, having everywhere the characteristics measured in a point close to the source) the dosimetric analysis indicates a substantial compliance according to both the 1998 and 2010 ICNIRP guidelines. Only in one case, related with the WPJ index in mother's brain, a more refined analysis is suggested to verify the compliance, considering a realistic spatial distribution of the impressed magnetic field.

The discussion of this case lets emerge a possible inconsistency in ICNIRP guidelines, evidenced in paragraph 3.3, related with the WPE index in the skin (particularly with poorly refined body models) and with the WPJ index in the spinal chord.

References

Andreuccetti, D., Zoppetti, N., 2006. Quasi-static electromagnetic dosimetry: from basic principles to examples of applications. International Journal of Occupational Safety and Ergonomics (JOSE) 12 (N.2), 201–215.

Cech, R., Leitgeb, N., Pediaditis, M., 2007. Fetal exposure to low frequency electric and magnetic fields. Physics in Medicine and Biology 32 (N.4), 879–888.

Christ, A., Kainz, W., Hahn, E.G., Honegger, K., Zefferer, M., Neufeld, E., Rascher, W., Janka, R., Bautz, W., Chen, J., Kiefer, B., Schmitt, P., Hollenbach, H.-P., Shen, J., Oberle, M., Szezerba, D., Kam, A., Guag, J.W., Kuster, N., 2010. The virtual family development of surface-based anatomical models of two adults and two children for dosimetric simulations. Physics in Medicine and Biology 55 (N.2), N23–N38.

Gabriel, S., Lau, R.W., Gabriel, C., 1996. The dielectric properties of biological tissues: III. Parametric models for the dielectric spectrum of tissues. Physics in Medicine and Biology 41 (N.11), 2271–2293.

Harris, F.J., 1978. On the use of windows for harmonic analysis with the discrete Fourier transform. Proceedings of the IEEE 66 (N.1), 51–83.

ICNIRP, 1998. Guidelines for limiting exposure to time-varying electric, magnetic, and electromagnetic fields (up to 300 GHz). Health Physics 74 (N.4), 494–522.

ICNIRP, 2003. Guidance on determining compliance of exposure to pulsed and complex non-sinusoidal waveforms below 100 kHz with ICNIRP guidelines. Health Physics 84 (N.3), 383–387.

ICNIRP, 2010. Guidelines for limiting exposure to time-varying electric and magnetic fields (1 Hz to 100 kHz). Health Physics 99 (N.6), 818–836.

Nagaoka, T., Togashi, T., Saito, K., Takahashi, M., Ito, K., Watanabe, S., 2007. An anatomically realistic whole-body pregnant-woman model and specific absorption rates for pregnant-woman exposure to electromagnetic plane waves from 10 MHz to 2 GHz. Physics in Medicine and Biology 52 (N.22), 6731–6745.

Oppenheim, A.V., Shafer, R.W., 2010. Discrete-time Signal Processing, third ed. Pearson. ISBN-13: 978-0-13-206709-6.

Zoppetti, N., Andreuccetti, D., 2009. Influence of the surface averaging procedure of the current density in assessing compliance with the ICNIRP low frequency basic restrictions by means of numerical techniques. Physics in Medicine and Biology 54 (N.15), 4835–4848.